Ultrahigh-Energy Cosmic Rays: Physics and Astrophysics at Extreme Energies

Günter Sigl

The origin of cosmic rays is one of the major unresolved questions in astrophysics. In particular, the highest energy cosmic rays observed have macroscopic energies up to several 10^{20} electron volts and thus provide a probe of physics and astrophysics at energies unattained in laboratory experiments. Theoretical explanations range from astrophysical acceleration of charged particles, to particle physics beyond the established standard model, and processes taking place at the earliest moments of our universe. Distinguishing between these scenarios requires detectors with effective areas in the 1000-square-kilometer range, which are now under construction or in the planning stage. Close connections with γ-ray and neutrino astrophysics add to the interdisciplinary character of this field.

High energy cosmic ray (CR) particles are shielded by Earth's atmosphere and reveal their existence on the ground only by indirect effects such as ionization and showers of secondary charged particles covering areas up to many km² for the highest energy particles. Indeed, in 1912 Victor Hess discovered CRs by measuring ionization from a balloon (*1*), and in 1938 Pierre Auger proved the existence of extensive air showers (EASs) caused by primary particles with energies above 10^{15} eV by simultaneously observing the arrival of secondary particles in ground detectors many meters apart (*2*).

After almost 90 years of research, the origin of CRs is still an open question, with a degree of uncertainty increasing with CR energy (*3*): Only below 100 MeV kinetic energy, where the solar wind shields protons coming from outside the solar system, must the sun give rise to the observed proton flux. Above that energy the CR spectrum exhibits little structure and is approximated by broken power laws $\propto E^{-\gamma}$ (Fig. 1): At the energy $E \simeq 4 \times 10^{15}$ eV, called the "knee," the flux of particles per area, time, solid angle, and energy steepens from a power law index $\gamma \simeq 2.7$ to one of index $\simeq 3.0$. The bulk of the CRs up to at least that energy are believed to originate within the Milky Way galaxy. Above the so called "ankle" at $E \simeq 5 \times 10^{18}$ eV, the spectrum flattens again to a power law of index $\gamma \simeq 2.8$. This latter feature is often interpreted as a crossover from a steeper galactic component, which above the ankle cannot be confined by the galactic magnetic field, to a harder component of extragalactic origin. At the highest energies there is no apparent end to the CR spectrum, and over the last few years giant air showers from CR primaries with energies exceeding 10^{20} eV (*4, 5*) (Fig. 2) have been detected. This repre-

sents up to 50 J in what appears to be one elementary particle, about 10^8 times higher than energies achievable in accelerator laboratories. The nature and origin of CRs above the ankle, which we will call ultrahigh-energy cosmic rays (UHECRs), and especially the ones above 10^{20} eV, are mysterious (*6, 7*) and will be the main focus of this review.

The conventional "bottom-up" scenario assumes that all high-energy charged particles are accelerated in astrophysical environments, typically in magnetized astrophysical shock waves. A general estimate of the maximal energy that can be achieved is given by the requirement that the gyroradius $r_g \simeq E/(ZeB)$ of the particle of charge Ze and energy E in a magnetic field B is smaller than the size R of the accelerator, in numbers

$$r_g \sim 100 Z^{-1} (E/10^{20}\ \text{eV})(B/\mu\text{G})^{-1}\ \text{kpc};$$
$$E \lesssim 10^{18} Z(R/\text{kpc})(B/\mu\text{G})\ \text{eV} \qquad (1)$$

Here, B is measured in microgauss (μG) and R in kiloparsec (1 pc = 3.09×10^{18} cm). Equation 1 is an optimistic estimate because it neglects the finite lifetime of the accelerator and energy losses due to interactions with the ambient environment such as synchrotron radiation in the magnetic field and production of secondary particles. Apart from the different scales, the maximal energy achievable in accelerator laboratories is also limited by their size and the magnetic field strength available for deflection. The remnants associated with galactic supernova explosions have sizes up to $R \sim$ pc with magnetic fields up to the milligauss range. According to Eq. 1 they should thus be able to accelerate CRs at least up to the knee, possibly up to the ankle. This and the fact that the power required to maintain the CR density in our galaxy is comparable to the kinetic energy output rate of galactic supernovae suggests that supernovae are the predominant sources of CRs in this energy range. Powerful extragalactic objects such as active galactic nu-

clei (AGN) (*8*) are envisaged to produce UHECRs (*3*). However, the existence of UHECRs at energies around 10^{20} eV and above, assuming them to be one of the known electromagnetically or strongly interacting particles, poses at least three theoretical problems discussed below.

Extragalactic Sources and the "GZK Cutoff"

Interactions with the omnipresent 2.7 K cosmic microwave background radiation (CMB), which is a thermal relic of the big bang, limit the attenuation length of the highest energy particles to less than about 50 megaparsecs (Mpc). For example, in the rest frame of a nucleon of energy $E \gtrsim E_{th}$ the CMB will appear as a background of γ-rays of sufficiently high energy to allow the production of pions. The threshold energy is given by

$$E_{th} = [m_\pi(m_N + m_\pi/2)]/$$
$$\epsilon \simeq 6.8 \times 10^{19}(\epsilon/10^{-3}\ \text{eV})^{-1}\ \text{eV} \qquad (2)$$

where m_N and m_π are the nucleon and pion mass, respectively, and $\epsilon \sim 10^{-3}$ eV is a typical CMB photon energy. For $E \gtrsim E_{th}$ the nucleon will loose a significant part of its energy on a length scale of $l_\pi \simeq 1/(\sigma_\pi n_{CMB}) \simeq 20$ Mpc, where $n_{CMB} \simeq 422$ cm^{-3} is the number density of CMB photons, and the pion production cross section $\sigma_\pi \sim 10^{-25}$ cm². Nuclei and γ-rays have similar energy loss distances owing to photodisintegration and electron-positron pair production on the CMB, respectively (*6*). Therefore, if the CR sources were all at cosmological distances (i.e., several thousand Mpc away), the energy spectrum would exhibit a depletion of particles above a few 10^{19} eV, the so-called Greisen-Zatsepin-Kuzmin (GZK) (*9*) cutoff. Because the data do not confirm such a cutoff (*4, 5*) (see Fig. 2), an astrophysical origin would require the sources to be within about 100 Mpc. The only way to avoid this conclusion without invoking an as yet unknown new physics is that charged particles accelerated in sources at much larger distances give rise to a secondary neutrino beam that can propagate unattenuated. This neutrino beam has to be sufficiently strong to produce the observed UHECRs within 100 Mpc by electroweak (EW) interactions with the relic neutrino background, the neutrino analog of the CMB (*10*). However, this requires powerful sources and local relic neutrino overdensities that are not consistent with commonly accepted ideas about the formation of the large-scale distri-

Institut d'Astrophysique de Paris, CNRS, 98bis Boulevard Arago, 75014 Paris, France. E-mail: sigl@iap.fr

bution of galaxies (*11*). In addition, to avoid excessive fluxes at lower energies, the sources have to be nearly opaque to γ-rays and nucleons (*11*).

The Maximal Acceleration Energy Problem

Evaluating the maximum energy estimates in Eq. 1 for known astrophysical objects demonstrates that only a few such objects are capable of accelerating charged particles up to a few 10^{20} eV (*12*). In our galactic neighborhood, pulsars with magnetic fields larger than 10^{12} G satisfy the criterion in Eq. 1 for iron nuclei. But it remains to be seen whether energy losses in the dense pulsar environment decrease the maximum energy below 10^{20} eV (*13*). Another suggestion is the acceleration of particles to such energies in ultrarelativistic jets from bipolar supernovae in our galaxy (*14*). In general, galactic sources tend to predict UHECR arrival directions correlated with galactic structures, which is not seen in the data (see below). Possible extragalactic accelerators include AGNs, radio galaxies (*15*), shock waves associated with large-scale structure formation (*16*), and possibly γ-ray bursts. AGNs are numerous enough, but are unlikely to reach the requisite energies, owing to strong energy losses in the intense radiation fields of their cores. Hot spots in the jets of radio galaxies are sufficiently tenuous to avoid excessive energy losses, and extend up to kpc scales. With magnetic fields in the milligauss regime, they meet the requirement of Eq. 1, and synchrotron observations suggest the presence of protons up to $\sim 10^{21}$ eV in these objects (*17*). The main problem is that such objects are rare (*15*). Gamma-ray bursts, another as yet not understood enigma of astrophysics, have been observed to occur
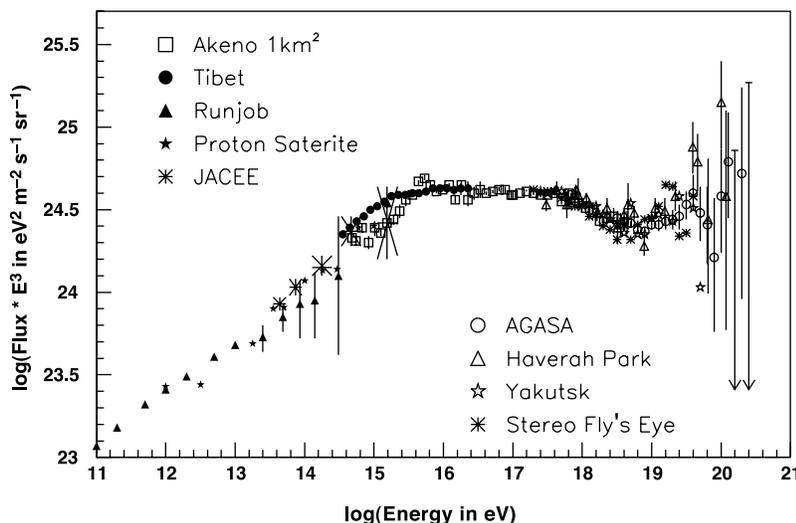
with a rate of about one burst within 100 Mpc (the maximal source distance for nucleons) per 100 years, each emitting up to $\sim 10^{54}$ ergs in γ-rays within a few seconds. Therefore, if γ-ray bursts are to explain the 20 or so UHECRs above 10^{20} eV observed within the past few decades, they have to meet the following requirements: They must emit at least as much energy in the form of UHECRs as in γ-rays in the MeV range; contrary to expectations, their rate must not correlate strongly with the star formation history (*18*); the UHECRs must be charged; and their arrival times must be spread out by at least a few hundred years (*19*). The latter requires large-scale magnetic fields that are stronger than about 10^{-10} G on Mpc scales (*20*).
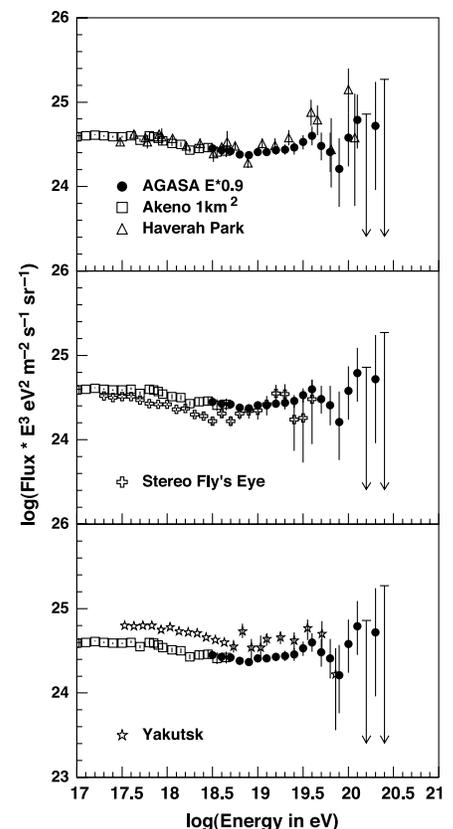
Angular Distributions and Missing Counterparts

The isotropy on large angular scales of UHECR arrival directions up to the highest energies (*21*) leaves only two possibilities for the source locations: There must be many nearby sources, at least one close to each arrival direction. Sufficiently powerful astrophysical accelerators that meet the above criteria are rare and should be detected within 100 Mpc, but no convincing source candidates have been found (*22*). Alternatively, there are a few nearby sources, which then requires strong deflection in galactic and/or extragalactic magnetic fields within a few Mpc propagation length. Equation 1 shows that this requires fields of at least $\sim 10^{-7}$ G on Mpc scales. Such high field strengths are expected to be localized in sheets and clusters of galaxies, but are hard to measure directly (*23*). These values are also close to upper limits established from independent observations such as the

frequency-dependent Faraday rotation of the polarization of radio emission from distant sources in intervening magnetic fields (*24*).

Whether the expected distribution and strength of magnetic fields associated with large-scale galaxy structure are consistent with UHECR spectra and angular distributions is currently under investigation (*25*). As an example (*26*), predictions for the distribution of arrival times and energies, the sky averaged spectrum, and the angular distribution of arrival directions in galactic coordinates for a specific model are shown in Fig. 3. In this scenario the UHECR sources are continuously distributed according to the matter density in the local supercluster, following an idealized pancake profile with scale height of 5 Mpc and scale length 20 Mpc, with no sources within 2 Mpc of the observer. All sources inject an $E^{-2.4}$ proton spectrum up to 10^{22} eV. The square of the magnetic field has a Kolmogorov spectrum with a maximal field strength $B_{max} = 5 \times 10^{-7}$ G in the plane center, and also follows the matter density. The observer is within 2 Mpc of the supergalactic plane and at a distance $d = 20$ Mpc from the plane center (Fig. 3). This example demonstrates the two major points of scenarios with large-scale fields up to a microgauss: First, a steepening of the UHECR spectrum

Fig. 2. The same as in Fig. 1, but focusing on the high-energy end above 10^{17} eV [from (*4*) with permission]. The "ankle" is again visible at $E \simeq 5 \times 10^{18}$ eV.

Fig. 1. The CR all-particle spectrum observed by different experiments above 10^{11} eV [from (*4*) with permission]. The differential flux in units of events per area, time, energy, and solid angle was multiplied by E^3 to project out the steeply falling character. The "knee" can be seen at $E \simeq 4 \times 10^{15}$ eV and the "ankle" at $E \simeq 5 \times 10^{18}$ eV.

in the diffusive regime below $\sim 10^{20}$ eV may help to explain the observed spectrum at least down to 10^{19} eV with only one source component (*27*). It is not clear, however, if the predicted flux is high enough above 10^{20} eV. Second, the predicted sky distribution may not be isotropic enough to be consistent with the data unless the sources are not correlated with the large-scale galaxy structure.

Whereas no significant UHECR anisotropy has so far been detected, the data suggest a possibly significant clustering on degree scales (*21*). This could indicate the presence of powerful discrete sources. To avoid dispersion of UHECRs of different energies from such discrete sources, the large-scale magnetic field then has to be smaller than $\sim 10^{-9}$ G (see Eq. 1) (*28*). Alternatively, lensing in magnetic fields of microgauss strength can also give rise to clustering (see, for example, the hot spots in the sky distribution in Fig. 3) (*26, 29*).

Generally, magnetic fields down to $\sim 10^{-11}$ G can leave observable imprints on UHECR arrival time, energy, and direction distributions (*6, 30*). This may also help to determine the origin of galactic and cosmological magnetic fields, which probably have been seeded in the early universe (*31*).

The enigma of UHECR origin is in a certain way opposite to the dark matter problem: Dark matter is expected to exist because of cosmological reasons (*32*) but has not yet

been found, whereas UHECRs above the GZK cutoff were not expected to exist but have been observed (*33*). In recent years this challenge triggered many theoretical proposals for the origin of these highest energy particles in the universe, as well as new experimental projects and the study of new detection concepts.

Pioneering Experiments and New Detection Concepts

Above $\sim 10^{14}$ eV, the showers of secondary particles created by interactions of the primary CRs in the atmosphere are extensive enough to be detectable from the ground. In the most traditional technique, charged hadronic particles, as well as electrons and muons in these EASs, are recorded by detecting the Cherenkov light that they emit when passing through water tanks, or by using scintillation counters. This technique was used by the ground-detector arrays at Volcano Ranch (*34*) in New Mexico, USA; at Haverah Park (*35*), UK; and at Yakutsk (*36*), Siberia, between the 1960s and 1980s. It is also used by the largest currently operating ground array, the Akeno Giant Air Shower Array (AGASA) near Tokyo, Japan, which covers an area of about 100 km^2 with about 100 detectors of a few meters in size, mutually separated by about 1 km (*37*). Given a flux of about one particle per km^2 per century above 10^{20} eV (see Fig. 2), the detection rate for such parti-

cles is less than one per year with such an instrument. The ground array technique allows one to measure a lateral cross section of the shower profile and to estimate the energy of the shower-initiating primary particle from the density of secondary charged particles.

EASs can also be detected by the nearly isotropic fluorescence emission of the nitrogen in the air that they excite. A system of mirrors and photomultipliers in the form of an insect's eye can be used to track the longitudinal development of EASs. This technique was first used by the Fly's Eye detector (*38*). The primary energy can be estimated from the total fluorescence yield and the longitudinal shower shape contains information about the primary composition. Comparison of CR spectra measured with the ground array and the fluorescence technique indicate systematic errors in energy calibration that are generally smaller than $\sim 40\%$ (*5*).

An upscaled version of the old Fly's Eye experiment, the High Resolution Fly's Eye detector, is looking for CRs in Utah, USA (*39*). Taking into account a duty cycle of about 10% because a fluorescence detector requires clear, moonless nights, this instrument will collect events above 10^{17} eV at a rate about 10 times larger than for the old Fly's Eye, corresponding to a few events above 10^{20} eV per year. Another project using the fluorescence technique is the Japanese Telescope Array (*40*), which is currently in
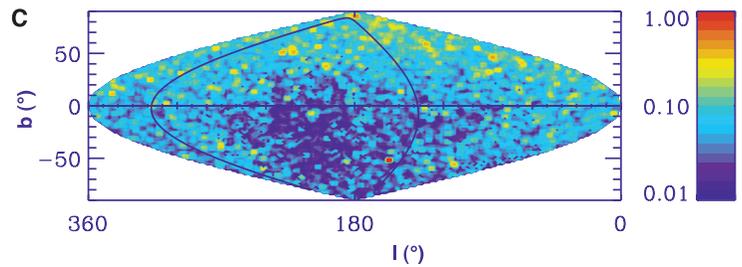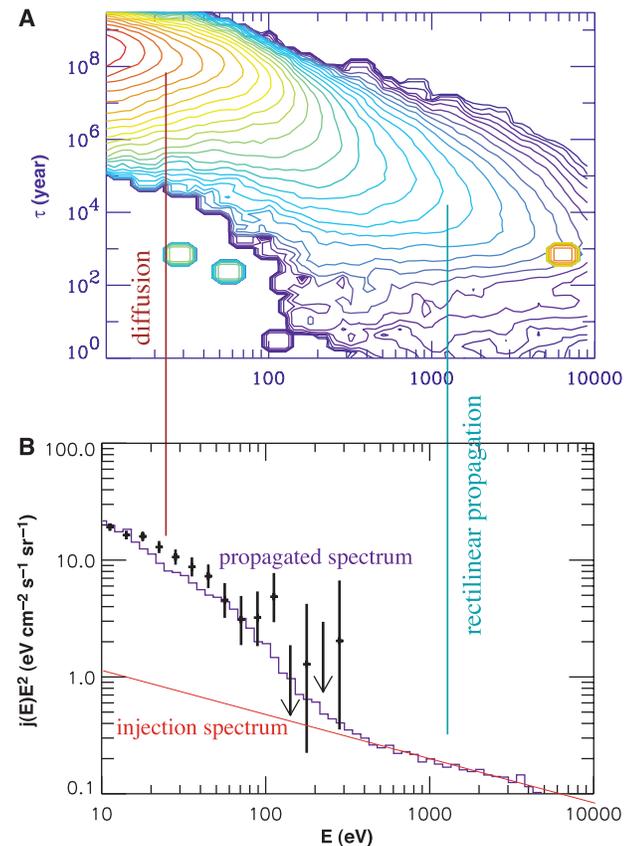
Fig. 3. The UHECR distribution of arrival times and energies (**A**), the sky averaged spectrum (**B**) [with 1σ error bars showing combined data from the Haverah Park (*35*), the Fly's Eye (*38*), and the AGASA (*37*) experiments above 10^{19} eV], and the sky distribution above 6×10^{19} eV versus galactic latitude (b) and longitude (l) (**C**) [color scale showing the intensity per solid angle for an angular resolution of 1.6°; supergalactic plane indicated in blue] in the bottom-up scenario with sources in the local supercluster of galaxies explained in the text. Twenty thousand proton trajectories for eight magnetic-field realizations each were calculated. The crossover from the diffusive regime below $\simeq 2 \times 10^{20}$ eV to the regime of rectilinear propagation at the highest energies can be seen in (A) and (B).

the proposal stage. If approved, its collecting power will also be about 10 times that of the old Fly's Eye above 10^{17} eV. The largest project presently under construction is the Pierre Auger Giant Array Observatory (*41*) planned for two sites, one in Mendoza, Argentina, and another in Utah, USA, for maximal sky coverage. Each site will have a 3000 km² ground array. The southern site will have about 1600 particle detectors (separated by 1.5 km each) overlooked by four fluorescence detectors. The ground arrays will have a duty cycle of nearly 100%, leading to detection rates about 30 times as large as that for the AGASA array, i.e., about 50 events per year above 10^{20} eV. About 10% of the events will be detected by both the ground array and the fluorescence component and can be used for cross calibration and detailed EAS studies. The detection energy threshold will be around 10^{18} eV.

There are also plans to detect EASs in the Earth's atmosphere from space. This would provide an increase by another factor of ~50 in collecting power compared with the Pierre Auger Project, i.e., an event rate above 10^{20} eV of up to a few thousand per year. Two concepts are currently being studied: the Orbiting Wide-angle Light-collector (OWL) (*42*) in the United States and the Extreme Universe Space Observatory (EUSO) (*43*) in Europe, a prototype of which may fly on the International Space Station.

Space-based detectors would be especially suitable for detection of very small event rates such as those caused by neutrino primaries, which rarely interact in the atmosphere owing to their small interaction cross sections. This disadvantage for the detection process is at the same time a blessing because it makes these elusive particles reach us unattenuated over cosmological distances and from very dense environments where all other particles (except gravitational waves) would be absorbed. Giving rise to showers typically starting deep within the atmosphere, they can also be distinguished from other primaries. In addition to detection from space, several other concepts are currently under study. These include detection of near-horizontal air showers with ground arrays (*44*), and detection of radio pulses emitted by neutrino-induced electromagnetic showers within large effective volumes [see (*6*) for more details].

Relics from the Early Universe

The apparent difficulties of bottom-up acceleration scenarios discussed earlier motivated the proposal of the "top-down" scenarios, where UHECRs, instead of being accelerated, are the decay products of certain sufficiently massive "X" particles produced by physical processes in the early universe. Furthermore, particle accelerator experiments and the mathematical structure of the standard model of the weak, electromagnetic, and strong in-

teractions suggest that these forces should be unified at energies of about 2×10^{16} GeV (1 GeV = 10^9 eV) (*45*), four to five orders of magnitude above the highest energies observed in CRs. The relevant "grand unified theories" (GUTs) predict the existence of X particles with mass m_X around the GUT scale of $\simeq 2 \times 10^{16}$ GeV. If their lifetime is comparable to or larger than the age of the universe, they would be dark-matter candidates, and their decays could contribute to UHECR fluxes today, with an anisotropy pattern that reflects the expected dark-matter distribution (*46*). However, in many GUTs, supermassive particles are expected to have lifetimes not much longer than their inverse mass, $\sim6.6 \times 10^{-41}(10^{16}$ GeV$/m_X)$ s, and thus have to be produced continuously if their decays are to give rise to UHECRs. This can only occur by emission from topological defects that are relics of cosmological phase transitions that could have occurred in the early universe at temperatures close to the GUT scale. Phase transitions in general are associated with a breakdown of a group of symmetries down to a subgroup that is indicated by an order parameter taking on a nonvanishing value. Topological defects occur between regions that are causally disconnected, such that the orientation of the order parameter cannot be communicated between these regions and thus will adopt different values. Examples are cosmic strings (*47*), magnetic monopoles (*48*), and domain walls (*49*). The Kibble mechanism states (*50*) that about one defect forms per maximal volume over which the order parameter can be communicated by physical processes. In the early universe the defect density is consequently given by the particle horizon, and their formation can by analogy be studied in solid-state experiments where the expansion rate of the universe corresponds to the quenching speed that is applied to induce the transition (*51*). The defects are topologically stable, but in the case of GUTs, time-dependent motion can lead to the emission of GUT-scale X particles.

One of the prime cosmological motivations to postulate inflation, a phase of exponential expansion in the early universe (*32*), was to dilute excessive production of "dangerous relics" such as topological defects and superheavy stable particles. However, directly after inflation, when the universe reheats, phase transitions can occur and such relics can be produced in cosmologically interesting abundances, and with a mass scale roughly given by the inflationary scale. This mass scale is fixed by the CMB anisotropies to $\sim10^{13}$ GeV (*52*), which is not far above the highest energies observed in CRs, thus motivating a connection between these primordial relics and UHECRs, which in turn may provide a probe of the early universe.

Within GUTs, the X particles typically

decay into jets of particles whose spectra can be estimated within the standard model. Before reaching Earth, the injected spectra are reprocessed by interactions with the low-energy photon backgrounds such as the CMB, and magnetic fields present in the universe [see (*6*, *53*) for details]. The UHECR spectrum expected in top-down scenarios (Fig. 4) shows that the observed flux can be reproduced above 3×10^{19} eV; at lower energies where the universe is transparent to nucleons, bottom-up mechanisms could explain the spectrum. The X-particle sources are not necessarily expected to be associated with astrophysical objects, but their distribution has to be sufficiently continuous to be consistent with observed UHECR angular distributions.

The most characteristic features of top-down models (Fig. 4) are as follows: Electromagnetic cascades induced by interactions of the injected particles with the low-energy photon backgrounds contribute to the diffuse γ-ray flux between 30 MeV and 100 GeV. This contribution is close to the flux measured by the EGRET detector flown on board the Compton γ-ray observatory satellite (*54*). The energy content in these γ-rays is comparable to that in the ultrahigh-energy neutrino flux, which should be detectable with next-generation experiments (Fig. 4). The neutrino flux is hardly influenced by subsequent interactions and thus directly represents the decay spectrum. In bottom-up scenarios, neutrinos can only be produced as secondaries, and for sources transparent to the primary nucleons, the neutrino flux must be smaller than in top-down scenarios (*55*). This can also serve as a discriminator between the top-down and bottom-up concepts. Finally, top-down models predict a significant γ-ray component above $\sim10^{20}$ eV, whereas nucleons would dominate at lower energies. This will be a strong discriminator because experiments will improve constraints on UHECR composition, which currently favor nucleons (*56*).

In addition to uncertainties in the shape and chemical composition of the spectrum, possibly the most significant shortcoming of top-down scenarios is their uncertainty in predicting the absolute flux normalization. At the least, the moderate rate of 10 decays per year in a spherical volume with radius equal to the Earth-sun distance, the rate necessary to explain the UHECR flux, is not in a remote corner of parameter space for most scenarios. Dimensional and scaling arguments imply that topological defects release X particles with an average rate at cosmic time t of

$$\dot{n}_X(t) = \kappa m_X{}^p t^{-4+p} \qquad (3)$$

where the dimensionless parameters κ and p depend on the specific top-down scenario (*6*). For example, hybrid defects involving cos-

mic strings have $p = 1$, and normalization of predicted spectra both at EGRET energies and around 10^{20} eV (Fig. 4) leads to $\kappa m_X \sim 10^{13}$ to 10^{14} GeV. For $\kappa \sim 1$, the resulting mass scale is again close to the inflation and GUT scales.

New Primary Particles and New Interactions

A possible way around the problem of missing counterparts in the framework of acceleration scenarios is to propose primary particles whose range is not limited by interactions with the CMB. The only established candidate is the neutrino. More speculatively, one could propose as yet undiscovered neutral particles that, according to Eq. 2, would have a higher GZK threshold if they were more massive than nucleons. In supersymmetric extensions of the standard model, new neutral hadronic bound states of light gluinos with quarks and gluons, so-called R-hadrons with masses in the 10-GeV range, have been suggested (*57*). However, this possibility is difficult to reconcile with accelerator constraints (*58*). Magnetic monopoles and their bound states (*59*) as well as superconducting string loops (*60*) similarly have the advantage of not being degraded significantly by interactions with the CMB and can be efficiently accelerated. The main problems with these primaries are the spectra; the atmospheric shower profiles; and for nonrelativistic monopoles, the arrival direction distributions. For example, the latter should show correlations with galactic structures, which are not observed. I will therefore focus on neutrinos as UHECR primaries.

To rescue the bottom-up scenario, the particle propagating over extragalactic distances, whether it is a neutrino or a new massive neutral hadron, has to be produced in interactions of a charged primary, which is accelerated in a powerful astrophysical object. In comparison to EASs induced by nucleons, nuclei, or γ-rays, the accelerator can now be located at cosmological distances. The cost of this conceptual advantage is an increase of the necessary charged primary energy to $\gtrsim 10^{22}$ eV owing to losses caused by the expansion of the universe and in the production of the secondary. These scenarios predict a correlation between UHECR arrival directions and sources at cosmological distances. Possible evidence for an angular correlation of events above the GZK cutoff with compact radio quasars at several thousand Mpc distance is being debated (*61*). A modest increase in data should determine whether or not there is a significant correlation.

Neutrino primaries have the advantage of being established particles. Unfortunately, within the standard model their interaction cross section with nucleons, $\sigma_{\nu N}$, falls short of producing ordinary air showers by about

five orders of magnitude, with significant ramifications for their detection, as mentioned above. However, at (squared) center of mass (CM) energies s above the EW scale, corresponding to $\simeq 10^{15}$ eV in the nucleon rest frame, this cross section has not been measured. Field theory constraints on the growth at higher energies based on conservation of reaction probabilities (*62*) are relatively weak (*63*). Neutrino-induced air showers above 10^{15} eV may therefore probe new physics beyond the EW scale, if it leads to enhanced cross sections.

One theoretical possibility consists of a large increase in the number of degrees of freedom above the EW scale (*64*). A specific implementation of this idea is provided by scenarios with additional large, compact dimensions and a string or quantum gravity scale $M_s \sim$ TeV ($= 10^{12}$ eV). This concept has received attention (*65*) because it may imply unification of all forces in the TeV range, not far above the scale of EW interactions. This scenario would avoid the "hierarchy problem" between the EW scale $\simeq 100$ GeV and the Planck scale $\simeq 10^{19}$ GeV of gravity. The cross sections within such scenarios have not been calculated from first

principles yet, but several arguments based on unitarity lead to estimates that can approximately be parameterized by (*66*)

$$\sigma_{new} \simeq 4\pi s/M_s^4$$
$$\simeq 10^{-27}(M_s/\text{TeV})^{-4}(E/10^{20}\text{ eV})\text{ cm}^2 \quad (4)$$

In the last expression E is the neutrino energy in the nucleon rest frame. A neutrino would typically start to interact in the atmosphere for $\sigma_{\nu N} \gtrsim 10^{-27}$ cm^2, i.e., in the case of Eq. 4 for $E \gtrsim 10^{20}$ eV, assuming $M_s \simeq 1$ TeV, a value consistent with lower limits from accelerator experiments (*67*) and astrophysical constraints (*68*) for four or more extra dimensions. The neutrino therefore becomes a primary candidate for the observed UHECR events (*69*). Cross sections of the form of Eq. 4 would predict the average atmospheric column depth of the first interaction point of neutrino-induced EASs to depend linearly on energy. This signature should be distinguishable from the logarithmic scaling expected for nucleons, nuclei, and γ-rays.

Independent of theoretical arguments, the UHECR data can be used to put constraints on neutrino cross sections at energies not accessible in the laboratory. Several experiments have not seen any air showers devel-

Fig. 4. All-particle spectra for a top-down model involving the decay into two quarks of nonrelativistic X particles of mass 10^{16} GeV, released from homogeneously distributed topological defects. The large-scale magnetic field was assumed to be $\lesssim 10^{-11}$ G. (**Bottom**) The fluxes of the "visible" particles, nucleons, and γ-rays. Error bars (1σ) are as in Fig. 3B (see also Fig. 2). Also shown are piecewise power-law fits to the observed charged CR flux below 10^{19} eV, the measurement of the diffuse γ-ray flux between 30 MeV and 100 GeV by the EGRET instrument (*54*), as well as upper limits on the diffuse γ-ray flux from various experiments at higher energies [see (*6*) for more details]. (**Top**) Neutrino fluxes. Shown are experimental neutrino flux limits from the Frejus underground detector (*73*), the Fly's Eye (*74*), the Goldstone radio telescope (*75*), and the Antarctic Muon and Neutrino Detector Array (AMANDA) neutrino telescope (*76*), as well as projected neutrino flux sensitivities of ICECUBE, the planned kilometer-scale extension of AMANDA (*77*), the Pierre Auger Project (*44*) (for electron and tau neutrinos separately), and the proposed space-based OWL (*42*) concept. Shown for comparison are the atmospheric neutrino background (hatched region marked "atmospheric"), and neutrino flux predictions for a model of AGN optically thick to nucleons ("AGN"), and for UHECR interactions with the CMB (*78*) ("Nγ"; dashed range indicating typical uncertainties for moderate source evolution). The top-down fluxes are shown for electron, muon, and tau neutrinos separately, assuming no (lower ν_τ curve) and maximal $\nu_\mu - \nu_\tau$ mixing (upper ν_τ curve, which would then equal the ν_μ flux), respectively.
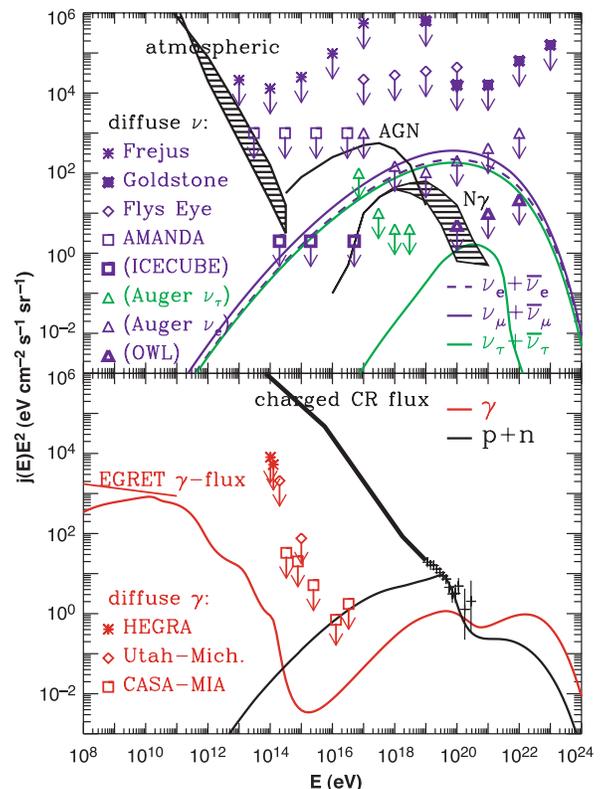
oping deep in the atmosphere and have put a limit on their rate (Fig. 4). The existence of a secondary neutrino flux from the decay of pions produced in UHECR interactions with the CMB ("$N\gamma$" in Fig. 4) then implies that $\sigma_{\nu N}$ cannot be larger than the standard model cross section by more than a factor of $\sim 10^3$ between 10^{18} and 10^{20} eV (70). This conclusion can only be avoided if UHECRs do not have an extragalactic origin or if $\sigma_{\nu N}$ is comparable to hadronic cross sections, giving rise to normal EASs. The projected sensitivity of future experiments such as the Pierre Auger Observatories and the space-based satellite projects (see Fig. 4) indicate that these cross-section limits could be improved by up to four orders of magnitude.

Probably the most radical proposition for the UHECR origin concerns a violation of one of the basic symmetry principles of modern field theory such as Lorentz invariance. Such violations can kinematically prevent energy-loss processes such as pion production at high Lorentz factors (71). A reliable experimental determination of source distances and primary composition could confirm such symmetry violations or constrain them possibly more strongly than accelerator experiments (72).

Conclusions

UHECRs attest to perhaps the most energetic processes in the universe. They are not only messengers of astrophysics at extreme energies, but may also open a window to particle physics beyond the standard model as well as probing processes occurring in the early universe at energies close to the GUT scale. Furthermore, complementary to other methods such as Faraday rotation measurements, UHECRs can be used to probe the poorly known large-scale cosmic magnetic fields and their origin. There is no single convincing theoretical model for the UHECR origin yet, and thus the solution to this problem will depend on detailed measurements of energy distributions, arrival directions and times, and composition.

References and Notes

1. V. F. Hess, *Phys. Z.* **13**, 1084 (1912).
2. P. Auger, R. Maze, T. Grivet-Meyer, *Acad. Sci.* **206**, 1721 (1938); P. Auger, R. Maze, *Acad. Sci.* **207**, 228 (1938).
3. For a general introduction on cosmic rays see, e.g., V. S. Berezinsky, S. V. Bulanov, V. A. Dogiel, V. L. Ginzburg, V. S. Ptuskin, *Astrophysics of Cosmic Rays* (North-Holland, Amsterdam, 1990); T. K. Gaisser, *Cosmic Rays and Particle Physics* (Cambridge Univ. Press, Cambridge, 1998).
4. M. Nagano, A. A. Watson, *Rev. Mod. Phys.* **72**, 689 (2000).
5. For a summary of the data situation and experimental issues see, e.g., S. Yoshida, H. Dai, *J. Phys. G* **24**, 905 (1998); X. Bertou, M. Boratav, A. Letessier-Selvon, *Int. J. Mod. Phys.* **A15**, 2181 (2000).
6. See, e.g., P. Bhattacharjee, G. Sigl, *Phys. Rep.* **327**, 109 (2000).
7. See, e.g., J. W. Cronin, *Rev. Mod. Phys.* **71**, S165 (1999); A. V. Olinto, *Phys. Rep.* **333-334**, 329 (2000); X. Bertou, M. Boratav, A. Letessier-Selvon, *Int. J. Mod. Phys.* **A15**, 2181 (2000).
8. Active galactic nuclei show highly variable electromagnetic emission at all energies up to the γ-ray regime. This emission is believed to be powered by accretion of gas and stars onto a black hole of between $\sim 10^6$ and $\sim 10^9$ solar masses in the center of the requisite galaxy. Galaxies with "dormant" cores such as the Milky Way are thought to be in stages of low accretion rates onto the central black hole.
9. K. Greisen, *Phys. Rev. Lett.* **16**, 748 (1966); G. T. Zatsepin, V. A. Kuzmin, *Pis'ma Zh. Eksp. Teor. Fiz.* **4**, 114 (1966) [*J. Exp. Theor. Phys. Lett.* **4**, 78 (1966)].
10. T. J. Weiler, *Phys. Rev. Lett.* **49**, 234 (1982); *Astrophys. J.* **285**, 495 (1984); *Astropart. Phys.* **11**, 317 (1999).
11. S. Yoshida, G. Sigl, S. Lee, *Phys. Rev. Lett.* **81**, 5505 (1998); J. J. Blanco-Pillado, R. A. Vázquez, E. Zas, *Phys. Rev. D* **61**, 123003 (2000).
12. A. M. Hillas, *Annu. Rev. Astron. Astrophys.* **22**, 425 (1984); C. A. Norman, D. B. Melrose, A. Achterberg, *Astrophys. J.* **454**, 60 (1995).
13. P. Blasi, R. I. Epstein, A. V. Olinto, *Astrophys. J. Lett.* **533**, L123 (2000).
14. A. Dar, R. Plaga, *Astron. Astrophys.* **349**, 259 (1999).
15. See, e.g., P. L. Biermann, *J. Phys. G Nucl. Part. Phys.* **23**, 1 (1997).
16. H. Kang, J. P. Rachen, P. L. Biermann, *Mon. Not. R. Soc. Astron.* **286**, 257 (1997).
17. P. L. Biermann, P. A. Strittmatter, *Astrophys. J.* **322**, 643 (1987).
18. F. Stecker, *Astropart. Phys.* **14**, 207 (2000). S. T. Scully, F. Stecker, http://xxx.lanl.gov/abs/astro-ph/0006112.
19. This assumes that γ-ray bursts emit isotropically. If, instead, the emission is beamed into a solid angle Ω, only a fraction $\Omega/(4\pi)$ of them would be visible in γ-rays, the energy release per burst would be smaller by the same factor, and the burst rate would be increased to $\sim 10^{-9}(4\pi/\Omega)$ Mpc^{-3} year^{-1}. This would reduce the necessary spread of arrival times by $\Omega/(4\pi)$.
20. E. Waxman, *Phys. Scr.* **T85**, 117 (2000).
21. N. Hayashida *et al.*, *Phys. Rev. Lett.* **77**, 1000 (1996); M. Takeda *et al.*, *Astrophys. J.* **522**, 225 (1999); N. Hayashida *et al.*, http://xxx.lanl.gov/abs/astro-ph/0008102.
22. G. Sigl, D. N. Schramm, P. Bhattacharjee, *Astropart. Phys.* **2**, 401 (1994); J. W. Elbert, P. Sommers, *Astrophys. J.* **441**, 151 (1995).
23. K. T. Kim *et al.*, *Nature* **341**, 720 (1989); T. Clark, P. P. Kronberg, H. Böhringer, http://xxx.lanl.gov/abs/astro-ph/0011281.
24. J. P. Vallee, *Fund. Cosm. Phys.* **19**, 1 (1997); P. Blasi, S. Burles, A. V. Olinto, *Astrophys. J.* **514**, L79 (1999).
25. G. Medina Tanco, *Astrophys. J. Lett.* **505**, L79 (1998); T. A. Ensslin, http://xxx.lanl.gov/abs/astro-ph/9906212; E.-J. Ahn, G. Medina-Tanco, P. L. Biermann, T. Stanev, http://xxx.lanl.gov/abs/astro-ph/9911123; G. R. Farrar, T. Piran, *Phys. Rev. Lett.* **84**, 3257 (2000); T. Stanev, R. Engel, A. Muecke, R. J. Protheroe, J. P. Rachen, *Phys. Rev. D* **62**, 093005 (2000).
26. M. Lemoine, G. Sigl, P. Biermann, http://xxx.lanl.gov/abs/astro-ph/9903124.
27. G. Sigl, M. Lemoine, P. Biermann, *Astropart. Phys.* **10**, 141 (1999); P. Blasi, A. V. Olinto, *Phys. Rev. D.* **59**, 023001 (1999).
28. G. Sigl, D. N. Schramm, S. Lee, C. T. Hill, *Proc. Natl. Acad. Sci. U.S.A.* **94**, 10501 (1997).
29. D. Harari, S. Mollerach, E. Roulet, *J. High-Energ. Phys.* **0002** 035 (2000); *J. High-Energy Phys.* **10**, 47 (2000).
30. G. Sigl, M. Lemoine, *Astropart. Phys.* **9**, 65 (1998).
31. See, e.g., D. Grasso, H. R. Rubinstein, http://xxx.lanl.gov/abs/astro-ph/0009061 (*Phys. Rep.*, in press).
32. See, e.g., E. W. Kolb, M. S. Turner, *The Early Universe* (Addison-Wesley, Redwood City, CA, 1990).
33. L. M. Celnikier, in *Proceedings of the 31st Rencontres de Moriond*, R. Ansari, Y. Giraud-Heraud, J. Tran Thanh Van, Eds. (Editions Frontieres, Gif-sur-Yvette, France, 1996), p. 453.
34. J. Linsley, *Phys. Rev. Lett.* **10** 146 (1963).
35. See, e.g., M. A. Lawrence, R. J. O. Reid, A. A. Watson, *J. Phys. G Nucl. Part. Phys.* **17**, 733 (1991); see also http://ast.leeds.ac.uk/haverah/havpark.shtml.
36. B. N. Afanasiev *et al.*, *Proceedings of the International Symposium on Extremely High Energy Cosmic Rays: Astrophysics and Future Observatories*, M. Nagano, Ed. (Institute for Cosmic Ray Research, Tokyo, 1996), p. 32.
37. N. Hayashida *et al.*, *Phys. Rev. Lett.* **73**, 3491 (1994); S. Yoshida *et al.*, *Astropart. Phys.* **3**, 105 (1995); M. Takeda *et al.*, *Phys. Rev. Lett.* **81**, 1163 (1998); see also www-akeno.icrr.u-tokyo.jp/AGASA/.
38. D. J. Bird *et al.*, *Phys. Rev. Lett.* **71**, 3401 (1993); *Astrophys. J.* **424**, 491 (1994); *Astrophys. J.* **441**, 144 (1995).
39. S. C. Corbató *et al.*, *Nucl. Phys. B* (*Proc. Suppl.*) **28B**, 36 (1992); see also http://hires.physics.utah.edu/.
40. M. Teshima *et al.*, *Nucl. Phys. B* (*Proc. Suppl.*) **28B**, 169 (1992); see also http://www-ta.icrr.u-tokyo.ac.jp/.
41. J. W. Cronin, *Nucl. Phys. B* (*Proc. Suppl.*) **28B**, 213 (1992); The Pierre Auger Observatory Design Report (ed. 2), March 1997; see also http://www.auger.org/ and http://www-lpnhep.in2p3.fr/auger/welcome.html.
42. D. B. Cline, F. W. Stecker, OWL/AirWatch science white paper, http://xxx.lanl.gov/abs/astro-ph/0003459; see also http://lheawww.gsfc.nasa.gov/docs/gamcosray/hecr/OWL/.
43. R. Benson, J. Linsley, *Southwest. Reg. Conf. Astron. and Astrophys.* **7**, 161 (1982); see also http://www.ifcai.pa.cnr.it/Ifcai/euso.html.
44. J. J. Blanco-Pillado, R. A. Vázquez, E. Zas, *Phys. Rev. Lett.* **78**, 3614 (1997); K. S. Capelle, J. W. Cronin, G. Parente, E. Zas, *Astropart. Phys.* **8**, 321 (1998); A. Letessier-Selvon, http://xxx.lanl.gov/abs/astro-ph/0009444.
45. See, e.g., S. Weinberg, *The Quantum Theory of Fields*, vol. 2, *Modern Applications* (Cambridge Univ. Press, Cambridge, 1996).
46. These models avoid the GZK cutoff because the UHECR flux is dominated by particle decays in the halo of our galaxy. However, in order to reproduce the observed UHECR flux, they require strong fine-tuning between the density in units of the critical density, Ω_x, and lifetime, t_x, of the X particle, $\Omega_x \sim 10^{-11}$ ($t_x/10^{10}$ years). Details of these scenarios have been discussed in V. Berezinsky, M. Kachelrieß, A. Vilenkin, *Phys. Rev. Lett.* **79**, 4302 (1997); V. A. Kuzmin, V. A. Rubakov, *Phys. Atom. Nucl.* **61**, 1028 (1998).
47. Strings correspond to the breakdown of rotational symmetry $U(1)$ around a certain direction; a laboratory example is vortices in superfluid helium.
48. Magnetic monopoles correspond to the breakdown of arbitrary three-dimensional rotations $SO(3)$ to rotations $U(1)$ around a specific direction.
49. Domain walls correspond to the breakdown of a discrete symmetry where the order parameter is only allowed to take several discrete values; a laboratory example is the Bloch walls separating regions of different magnetization along the principal axis of a ferromagnet.
50. Reviewed in T. W. B. Kibble, *J. Phys.* **A9**, 1387 (1976); A. Vilenkin, *Phys. Rep.* **121**, 263 (1985).
51. See, e.g., T. Vachaspati, *Contemp. Phys.* **39**, 225 (1998); W. Zurek, *Phys. Rep.* **276**, 177 (1996).
52. For a brief review see V. Kuzmin, I. Tkachev, *Phys. Rep.* **320**, 199 (1999).
53. G. Sigl, S. Lee, P. Bhattacharjee, S. Yoshida, *Phys. Rev. D* **59**, 043504 (1999).
54. P. Sreekumar *et al.*, *Astrophys. J.* **494**, 523 (1998).
55. E. Waxman, J. Bahcall, *Phys. Rev. D* **59**, 023002 (1999); J. Bahcall, E. Waxman, http://xxx.lanl.gov/abs/hep-ph/9902383; K. Mannheim, R. J. Protheroe, J. P. Rachen, http://xxx.lanl.gov/abs/astro-ph/9812398; J. P. Rachen, R. J. Protheroe, K. Mannheim, http://xxx.lanl.gov/abs/astro-ph/9908031.
56. F. Halzen, R. A. V'azques, T. Stanev, H. P. Vankov, *Astropart. Phys.* **3**, 151 (1995); M. Ave, J. A. Hinton, R. A. V'azques, A. A. Watson, E. Zas, *Phys. Rev. Lett.* **85** 2244 (2000).
57. G. R. Farrar, *Phys. Rev. Lett.* **76**, 4111 (1996); D. J. H. Chung, G. R. Farrar, E. W. Kolb, *Phys. Rev. D* **57**, 4696 (1998).
58. I. F. Albuquerque *et al.* (E761 collaboration), *Phys. Rev. Lett.* **78**, 3252 (1997); A. Alavi-Harati *et al.*

(KTeV collaboration), *Phys. Rev. Lett.* **83**, 2128 (1999).

59. See S. D. Wick, T. W. Kephart, T. J. Weiler, P. L. Biermann, http://xxx.lanl.gov/abs/astro-ph/0001233.
60. S. Bonazzola, P. Peter, *Astropart. Phys.* **7**, 161 (1997).
61. G. R. Farrar, P. L. Biermann, *Phys. Rev. Lett.* **81**, 3579 (1998); C. M. Hoffman, *Phys. Rev. Lett.* **83**, 2471 (1999); G. R. Farrar, P. L. Biermann, *Phys. Rev. Lett.* **83**, 2472 (1999); G. Sigl, D. F. Torres, L. A. Anchordoqui, G. E. Romero, http://xxx.lanl.gov/abs/astro-ph/0008363; A. Virmani *et al.*, http://xxx.lanl.gov/abs/astro-ph/0010235.
62. The technical term in quantum field theory is "unitarity."
63. H. Goldberg, T. J. Weiler, *Phys. Rev. D* **59**, 113005 (1999).
64. G. Domokos, S. Kovesi-Domokos, *Phys. Rev. Lett.* **82**, 1366 (1999).
65. See, e.g., N. Arkani-Hamed, S. Dimopoulos, G. Dvali, *Phys. Rev. D* **59**, 086004 (1999).
66. S. Nussinov, R. Shrock, *Phys. Rev. D* **59**, 105002 (1999);

P. Jain, D. W. McKay, S. Panda, J. P. Ralston, *Phys. Lett.* **B484**, 267 (2000); J. P. Ralston, P. Jain, D. W. McKay, S. Panda, http://xxx.lanl.gov/abs/hep-ph/0008153.
67. See, e.g., S. Cullen, M. Perelstein, M. E. Peskin, *Phys. Rev.D* **62**, 055012 (2000).
68. S. Cullen, M. Perelstein, *Phys. Rev. Lett.* **83**, 268 (1999); V. Barger, T. Han, C. Kao, R.-J. Zhang, *Phys. Lett. B* **461**, 34 (1999).
69. To give rise to the EASs so far observed, however, cross sections of at least a few 10^{-26} cm² are necessary; see M. Kachelrieß, M. Plümacher, *Phys. Rev. D* **62**, 103006 (2000); L. Anchordoqui *et al.*, http://xxx.lanl.gov/abs/0011097.
70. C. Tyler, A. V. Olinto, G. Sigl, http://xxx.lanl.gov/abs/hep-ph/0002257 (*Phys. Rev. D.*, in press).
71. See, e.g., S. Coleman, S. L. Glashow, *Nucl. Phys.* **B574**, 130 (2000); L. Gonzalez-Mestres, *Nucl. Phys. B* (*Proc. Suppl.*) **48**, 131 (1996).
72. See, e.g., R. Aloisio, P. Blasi, P. L. Ghia, A. F. Grillo, *Phys. Rev. D* **62**, 053010 (2000).

73. W. Rhode *et al.*, *Astropart. Phys.* **4**, 217 (1996).
74. R. M. Baltrusaitis *et al.*, *Astrophys. J.* **281**, L9 (1984); *Phys. Rev. D* **31**, 2192 (1985).
75. P. W. Gorham, K. M. Liewer, C. J. Naudet, http://xxx.lanl.gov/abs/astro-ph/9906504.
76. For general information see http://amanda.berkeley.edu/; see also F. Halzen, *New Astron. Rev.* **42**, 289 (1999).
77. For general information see http://www.ps.uci.edu/icecube/workshop.html; see also F. Halzen, *Am. Astron. Soc. Meet.* **192**, 62 28 (1998); AMANDA collaboration, talk presented at the 8th International Workshop on Neutrino Telescopes, Venice, February 1999, http://xxx.lanl.gov/abs/astro-ph/9906205.
78. R. J. Protheroe, P. A. Johnson, *Astropart. Phys.* **4**, 253 (1996); [erratum] *Astropart. Phys.* **5**, 215 (1996).
79. I acknowledge P. Biermann, P. Blasi, M. Boratav, T. Ensslin, P. Peter, R. Plaga, G. Raffelt, and A. Watson for helpful comments on the manuscript.

REVIEW

Gamma-Ray Bursts: Accumulating Afterglow Implications, Progenitor Clues, and Prospects

P. Mészáros

Gamma-ray bursts (GRBs) are sudden, intense flashes of gamma rays that, for a few blinding seconds, light up in an otherwise fairly dark gamma-ray sky. They are detected at the rate of about once a day, and while they are on, they outshine every other gamma-ray source in the sky, including the sun. Major advances have been made in the last 3 or 4 years, including the discovery of slowly fading x-ray, optical, and radio afterglows of GRBs, the identification of host galaxies at cosmological distances, and evidence showing that many GRBs are associated with star-forming regions and possibly supernovae. Progress has been made in understanding how the GRB and afterglow radiation arises in terms of a relativistic fireball shock model. These advances have opened new vistas and questions on the nature of the central engine, the identity of their progenitors, the effects of the environment, and their possible gravitational wave, cosmic ray, and neutrino luminosity. The debates on these issues indicate that GRBs remain among the most mysterious puzzles in astrophysics.

Until a few years ago, GRBs were known predominantly as bursts of γ-rays, largely devoid of any observable traces at any other wavelengths. However, a striking development in the last several years has been the measurement and localization of fading x-ray signals from some GRBs, lasting typically for days and making possible the optical and radio detection of afterglows, which, as fading beacons, mark the location of the fiery and brief GRB event. These afterglows in turn enabled the measurement of redshift distances, the identification of host galaxies, and the confirmation that GRBs were, as suspected, at cosmological distances on the order of billions of light years, similar to those of the most distant galaxies and quasars. Even at those distances, they appear so bright that

their energy output must be on the order of 10^{51} to 10^{54} erg s^{-1}, larger than that of any other type of source. It is comparable to burning up the entire mass-energy of the sun in a few tens of seconds, or to emit over that same period of time as much energy as our entire Milky Way does in a hundred years.

GRBs were first reported in 1973 on the basis of 1969–1971 observations by the Vela military satellites monitoring for nuclear explosions in verification of the Nuclear Test Ban Treaty. When these mysterious γ-ray flashes, which did not come from Earth's direction, were initially detected, the first suspicion (quickly abandoned) was that they might be the product of an advanced extraterrestrial civilization. Soon, however, it was realized that this was a new and extremely puzzling cosmic phenomenon. For the next 20 years, hundreds of GRB detections were made, and frustratingly, they continued to vanish too soon to get an accurate angular position to permit any follow-up observations. The reason for this is that γ-rays are

notoriously hard to focus, so γ-ray images are generally not very sharp.

The next major advance occurred in 1991 with the launch of the Compton Gamma-Ray Observatory (CGRO), whose results have been summarized in (*1*). The all-sky survey from the Burst and Transient Experiment (BATSE) onboard CGRO, which measured about 3000 bursts, showed that they were isotropically distributed, suggesting a cosmological distribution with no dipole and quadrupole components. The spectra were nonthermal, the number of photons per unit photon energy varying typically as $N(\varepsilon) \propto \varepsilon^{-\alpha}$, where $\alpha \sim 1$ at low energies changes to $\alpha \sim 2$ to 3 above a photon energy $\varepsilon_0 \sim 0.1$ to 1 MeV (*2*), the spectral power law dependence extending sometimes to GeV energies (*3*). The durations (at MeV energies) range from 10^{-3} s to about 10^3 s, with a roughly bimodal distribution of long bursts (duration $t_b \gtrsim 2$ s) and short bursts ($t_b \lesssim 2$ s) (*4*), and substructure sometimes down to milliseconds. The γ-ray light curves range from smooth, fast-rise and quasi-exponential decay, through curves with several peaks, to variable curves with many peaks (Fig. 1). The pulse distribution is complex, and the time histories of the emission as a function of energy can provide clues for the geometry of the emitting regions (*5*).

A watershed event occurred in 1997, when the Italian-Dutch satellite BeppoSAX succeeded in obtaining high-resolution x-ray images (*6*) of the predicted fading afterglow of GRB970228, followed by a number of other detections at an approximate rate of 10 per year (Fig. 2). These detections, after a 4- to 6-hour delay for processing, led to positions accurate to about an arc minute, which allowed the detection and follow-up of the afterglows at optical and longer wavelengths [e.g., (*7*)]. This paved

Department of Astronomy and Astrophysics, Pennsylvania State University, University Park, PA 16803, USA, and Institute for Theoretical Physics, University of California, Santa Barbara, CA 93106, USA. E-mail: pmeszaros@astro.psu.edu

Science

Ultrahigh-Energy Cosmic Rays: Physics and Astrophysics at Extreme Energies
Günter Sigl

View the article online
Permissions